

# Online Parallel Accumulation–Serial Fragmentation (PASEF) with a Novel Trapped Ion Mobility Mass Spectrometer

## Authors

Florian Meier, Andreas-David Brunner, Scarlet Koch, Heiner Koch, Markus Lubeck, Michael Krause, Niels Goedecke, Jens Decker, Thomas Kosinski, Melvin A. Park, Nicolai Bache, Ole Hoerning, Jürgen Cox, Oliver Rätther, and Matthias Mann

## Correspondence

mman@biochem.mpg.de

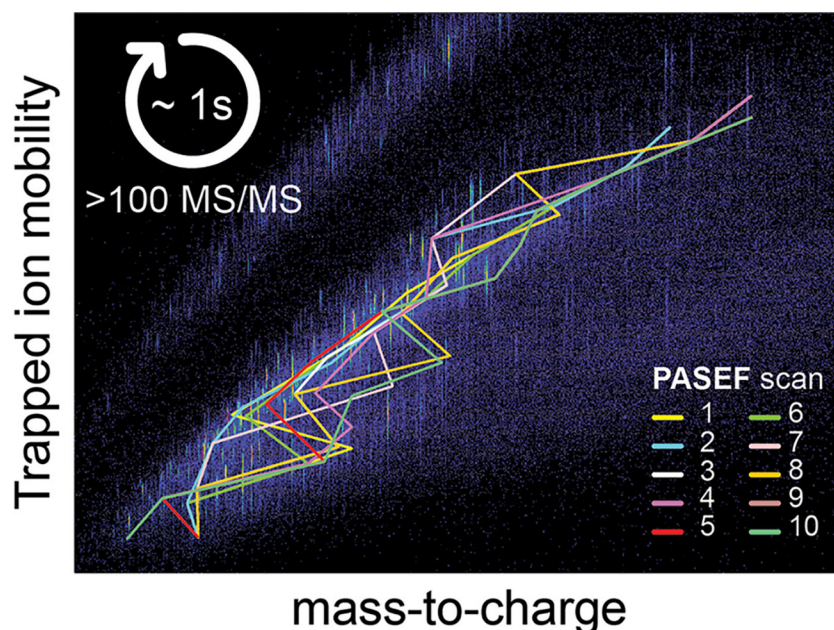
## In Brief

PASEF multiplies the sequencing speed without any loss in sensitivity and is implemented in the timsTOF Pro instrument introduced here. Sequencing speeds above 100 Hz enable single run proteome analysis at a depth of 6000 proteins, making the instrument particularly attractive for rapid and highly sensitive proteomics. Collisional cross sections can be determined with up to 0.1% precision and acquired on a scale of 100,000s, which opens exciting areas for proteomics exploration.

## Highlights

- Online PASEF achieves greater than 100 MS/MS per second at full sensitivity.
- Accurate label-free quantification of over 6000 proteins in 2 h.
- High throughput demonstrated on 50 ng digests measured in 5 min.
- High-precision determination of 100,000 peptide collisional cross sections.

## Graphical Abstract





# Online Parallel Accumulation–Serial Fragmentation (PASEF) with a Novel Trapped Ion Mobility Mass Spectrometer\*<sup>§</sup>

✉ Florian Meier‡, Andreas-David Brunner‡, Scarlet Koch§, Heiner Koch§, Markus Lubeck§, Michael Krause§, Niels Goedecke§, Jens Decker§, Thomas Kosinski§, Melvin A. Park¶, Nicolai Bache||, Ole Hoerning||, Jürgen Cox\*\*, Oliver Rätther§, and ✉ Matthias Mann‡‡§§

In bottom-up proteomics, peptides are separated by liquid chromatography with elution peak widths in the range of seconds, whereas mass spectra are acquired in about 100 microseconds with time-of-flight (TOF) instruments. This allows adding ion mobility as a third dimension of separation. Among several formats, trapped ion mobility spectrometry (TIMS) is attractive because of its small size, low voltage requirements and high efficiency of ion utilization. We have recently demonstrated a scan mode termed parallel accumulation - serial fragmentation (PASEF), which multiplies the sequencing speed without any loss in sensitivity (Meier *et al.*, PMID: 26538118). Here we introduce the timsTOF Pro instrument, which optimally implements online PASEF. It features an orthogonal ion path into the ion mobility device, limiting the amount of debris entering the instrument and making it very robust in daily operation. We investigate different precursor selection schemes for shotgun proteomics to optimally allocate in excess of 100 fragmentation events per second. More than 600,000 fragmentation spectra in standard 120 min LC runs are achievable, which can be used for near exhaustive precursor selection in complex mixtures or accumulating the signal of weak precursors. In 120 min single runs of HeLa digest, MaxQuant identified more than 6,000 proteins without matching to a library and with high quantitative reproducibility ( $R > 0.97$ ). Online PASEF achieves a remarkable sensitivity with more than 2,500 proteins identified in 30 min runs of only 10 ng HeLa digest. We also show that highly reproducible collisional cross sections can be acquired on a large scale ( $R > 0.99$ ). PASEF on the timsTOF Pro is a valuable addition to the technological toolbox in proteomics, with a number of unique operating modes that are only beginning to be explored. *Molecular & Cellular Proteomics* 17: 2534–2545, 2018. DOI: 10.1074/mcp.TIR118.000900.

Jointly, proteins form a cellular machinery—the proteome—that orchestrates essentially all biological processes in health and disease. Studying it on a system-wide scale holds great promise to advance our understanding of cellular biology and disease mechanisms (1–3). However, as compared with genomics and transcriptomics technologies, proteomics still lags in terms of coverage, throughput, and sensitivity. Virtually complete measurements of mammalian proteomes have become possible (4), but have mostly involved laborious sample preparation workflows, days of measurement time and substantial amounts of starting material. Furthermore, current high-performance instrumentation often requires expert knowledge and extensive maintenance, which impedes widespread adaptation of proteomics in nonspecialized laboratories.

In bottom-up workflows, proteins are extracted from a biological sample of interest and enzymatically cleaved to make them more amenable to mass spectrometric (MS) analysis. The resulting complex peptide mixtures are typically separated via nano-flow liquid chromatography (LC)<sup>1</sup>, ionized by electrospray and mass analyzed. In “data-dependent” or “topN” acquisition schemes, the mass spectrometer detects suitable peptide precursor ions in full scans (MS) and selects them for fragmentation in *N* consecutive MS/MS scans. High resolution and high mass accuracy analyzers detect hundreds of thousands of distinct molecular features in single LC-MS experiments, of which only a minority is identified and quantified (5). These co-eluting peptides with abundances ranging over many orders of magnitude present a formidable analytical challenge, which has constantly pushed the development of faster and more sensitive instrumentation over the last decades (1, 3, 6, 7).

From the ‡Proteomics and Signal Transduction, Max Planck Institute of Biochemistry, Am Klopferspitz 18, 82152 Martinsried, Germany; §Bruker Daltonik GmbH, Fahrenheitstr. 4, 28359 Bremen, Germany; ¶Bruker Daltonics Inc., Manning Road, Billerica, Massachusetts 01821; ||Evosep Biosystems, Thriges Pl. 6, 5000 Odense, Denmark; \*\*Computational Systems Biochemistry, Max Planck Institute of Biochemistry, Am Klopferspitz 18, 82152 Martinsried, Germany; ‡‡NNF Center for Protein Research, Faculty of Health Sciences, University of Copenhagen, Blegdamsvej 3B, 2200 Copenhagen, Denmark

✂ Author's Choice—Final version open access under the terms of the Creative Commons CC-BY license.

Received June 4, 2018, and in revised form, October 30, 2018

Published, MCP Papers in Press, November 1, 2018, DOI 10.1074/mcp.TIR118.000900

Time-of-flight (TOF) instruments have several very desirable properties for the analysis of complex peptide mixtures and have consequently been employed in shotgun proteomics for a long time (8, 9). Instrumental performance has steadily improved over the years, and our groups have described shotgun proteome measurements at a mass resolution of more than 35,000 within about 100  $\mu$ s on the *impact II* (10), the predecessor of the instrument that is the subject of this paper. The high acquisition rate of TOF instruments allows coupling them with very fast separation techniques, such as ion mobility spectrometry (IMS) (11–13). IMS separates ions in the gas phase based on their size and shape, or more precisely their collisional cross section (CCS,  $\Omega$ ), typically within 10s to 100s of milliseconds (14). As the ions emerge from the IMS device, they can be efficiently sampled in the ms or sub-ms time frame with TOF analyzers. Nested between LC and MS, the technology provides an additional dimension of separation (15–17) and can increase analysis speed and selectivity (18), also with highly complex proteomics samples (19–23). However, many implementations of IMS, such as drift tubes, are challenging because of the device sizes and high voltages involved and may also limit the proportion of the continuous incoming beam that can be utilized (12, 13, 24). Trapped ion mobility spectrometry (TIMS) (25, 26) reverses the concept of traditional drift tube ion mobility by bringing ions to a rest at different positions in an ion tunnel device, balanced in an electrical field against a constant gas stream (27). Once enough ions have been trapped and separated, lowering the electrical potential releases time-resolved ions from the TIMS device into the downstream mass analyzer. This design reduces the IMS analyzer dimensions to about 10 centimeters in length—allowing two of them to be implemented in series for 100% duty cycle operation (28). TIMS furthermore offers high flexibility in that users can tune the ion mobility resolving power ( $\Omega/\Delta_{FWHM}\Omega$ ) up to 200 or higher by simply lowering the TIMS scan speed (29, 30).

We have recently introduced “Parallel Accumulation - SERIAL Fragmentation” (PASEF) (31), which synchronizes MS/MS precursor selection with TIMS separation. This acquisition scheme allows fragmentation of more than one precursor per TIMS scan and we demonstrated that PASEF increases the sequencing speed severalfold without loss of sensitivity. As precursor ions are accumulated in parallel, PASEF overcomes the diminishing returns of increasingly fast MS/MS acquisition, which otherwise necessarily implied less and less ions per spectrum. Our first iteration was implemented on a laboratory prototype, which required manual precursor programming and was limited by the speed of the electronics involved. Here, we describe the construction and investigate the pro-

teomics performance of the first mass spectrometer that fully integrates the PASEF concept, the Bruker *timsTOF Pro*.

#### EXPERIMENTAL PROCEDURES

**Cell Culture and Sample Preparation**—Human cervical cancer cells (HeLa S3, ATCC, Manassas, VA) were grown in Dulbecco’s modified Eagle’s medium with 10% fetal bovine serum, 20 mM glutamine and 1% penicillin-streptomycin (all Life Technologies Ltd., Paisley, UK). *Escherichia coli* (strain: XL1 blue) was cultured at 37 °C in LB medium until logarithmic phase (optical density = 0.5,  $\lambda$  = 600 nm). Cells were collected by centrifugation. Following a washing step with cold phosphate buffered saline, they were pelleted and flash frozen in liquid nitrogen and stored at –80 °C.

One-device cell lysis, reduction, and alkylation was performed in sodium deoxycholate (SDC) buffer with chloroacetamide (PreOmics GmbH, Martinsried, Germany) according to our previously published protocol (32). Briefly, the cell suspension was twice boiled for 10 min at 95 °C and subsequently sonicated for 15 min at maximum energy (Bioruptor, Diagenode, Seraing, Belgium). Proteins were enzymatically hydrolyzed overnight at 37 °C by LysC and trypsin (1:100 enzyme:protein (wt/wt) for both). To stop the digestion, the reaction mixture was acidified with five volumes of isopropanol with 1% trifluoroacetic acid (TFA). Peptides were de-salted and purified in two steps, first on styrenedivinylbenzene-reversed phase sulfonate (SDB-RPS), and second on  $C_{18}$  sorbent. The dried eluates were re-constituted in water with 2% acetonitrile (ACN) and 0.1% TFA for direct LC-MS analysis or high pH reversed-phase fractionation.

For the experiments with the Evosep One (see below), HeLa cell pellets were re-suspended and lysed in water/trifluoroethanol. Disulfide bonds were reduced with dithiothreitol and alkylated with iodoacetamide in ammonium bicarbonate buffer. Following tryptic digestion, the peptide mixture was de-salted and purified on  $C_{18}$  sorbent.

**Peptide Fractionation**—High pH reversed-phase fractionation was performed on an EASY-nLC 1000 (Thermo Fisher Scientific, Bremen, Germany) coupled to a “spider fractionator” (PreOmics) as detailed in ref (33). Purified peptides were separated on a 30 cm  $\times$  250  $\mu$ m reversed-phase column (PreOmics) at a flow rate of 2  $\mu$ l/min at pH 10. The binary gradient started from 3% buffer B (PreOmics), followed by linear increases to first 30% B within 45 min, to 60% B within 17 min, and finally to 95% B within 5 min. Each sample was automatically concatenated into 48 fractions in 90 s time intervals. The fractions were dried in a vacuum-centrifuge and reconstituted in water with 2% ACN and 0.1% TFA for LC-MS analysis.

**Liquid Chromatography**—An EASY-nLC 1200 (Thermo Fisher Scientific) ultra-high pressure nano-flow chromatography system was coupled online to a hybrid trapped ion mobility spectrometry - quadrupole time of flight mass spectrometer (*timsTOF Pro*, Bruker Daltonics, Bremen, Germany) with a modified nano-electrospray ion source (10) (CaptiveSpray, Bruker Daltonics). Liquid chromatography was performed at 60 °C and with a constant flow of 400 nL/min on a reversed-phase column (50 cm  $\times$  75  $\mu$ m i.d.) with a pulled emitter tip, packed with 1.9  $\mu$ m  $C_{18}$ -coated porous silica beads (Dr. Maisch, Ammerbuch-Entringen, Germany). Mobile phases A and B were water with 0.1% formic acid (v/v) and 80/20/0.1% ACN/water/formic acid (v/v/vol), respectively. In 120-min experiments, peptides were separated with a linear gradient from 7.5 to 27.5% B within 60 min, followed by an increase to 37.5% B within 30 min and further to 55% within 10 min, followed by a washing step at 95% B and re-equilibration. In 60 min separations, the gradient increased from 10 to 30% B within 30 min, followed by an increase to 40% B within 15 min and further to 57.5% B within 5 min before washing and re-equilibration. In 30 min separations, the initial 10–30% B step was 15 min, followed by a linear increase to 40% B (7.5 min) and 57.5% B (2.5 min) before washing and re-equilibration.

<sup>1</sup> The abbreviations used are: LC, liquid chromatography; CCS, collisional cross section; IMS, ion mobility spectrometry; PASEF, parallel accumulation–serial fragmentation; TIMS, trapped ion mobility spectrometry.

For some experiments we used the Evosep One (Evosep, Odense, Denmark), a new HPLC instrument employing an embedded gradient and capable of fast turnaround between analyses (34). Samples were eluted from Evtips at low pressure into the storage loop with a gradient offset to lower the percentage of organic buffer. Separation was performed on a customized 5.6 min gradient (200 samples/day method) at a flow rate of 2.0  $\mu\text{l}/\text{min}$  on a 4 cm x 150  $\mu\text{m}$  i.d. reversed-phase column packed with 3  $\mu\text{m}$  C<sub>18</sub>-coated porous silica beads (PepSep, Odense, Denmark).

**The timsTOF Pro Mass Spectrometer**—The *timsTOF Pro* is the successor to the *impact II* instrument, compared with which it features an additional ion mobility analyzer. However, the *timsTOF Pro* is a complete redesign in hardware and firmware. Apart from incorporating TIMS, the design goals included the achievement of similar or better mass resolution (>35,000) and improved robustness through a modified ion path.

In the experiments described here, the mass spectrometer was operated in PASEF mode. Desolvated ions entered the vacuum region through the glass capillary and were deflected by 90°, focused in an electrodynamic funnel, and trapped in the front region of the TIMS tunnel consisting of stacked printed circuit boards (PCBs) with an inner diameter of 8 mm and a total length of 100 mm. The PCB electrodes form a stacked multipole in the direction of ion transfer, in which an applied RF potential of 350 V<sub>pp</sub> confined the trapped ions radially. The TIMS tunnel is electrically separated into two parts (dual TIMS), where the first region is operated as an ion accumulation trap that primarily stores all ions entering the mass spectrometer, while the second part performs trapped ion mobility analysis (28). As soon as the TIMS analysis is finished, all stored ions are transferred to the analyzer part and the storage region is filled again. If equal accumulation and analysis times are used in both TIMS regions, this enables operation at duty cycles close to 100%. Ion transfer between the two regions takes 2 ms and therefore does not affect the overall ion utilization for typical ramp and accumulation times around 25 to 200 ms.

In both TIMS regions, the RF field is superimposed (from entrance to exit) by an increasing longitudinal electrical field gradient, such that ions in the tunnel simultaneously experience a drag from the incoming gas flow through the capillary and a repulsion from the electrical field. Here, we used a flow of ambient laboratory air for ion mobility separation. Depending on their collisional cross sections and charge states, ions come to rest closer to the entrance of the tunnel (high ion mobility) or closer to its exit (low ion mobility). Trapped ion mobility separation was achieved by ramping the entrance potential of the second TIMS region from -207 V to -77 V. A single TIMS-MS scan is composed of many individual TOF scans of about 110  $\mu\text{s}$  each. In the experiments reported here, we first systematically varied the ramp times from 25, 50, 100, 150, to 200 ms while keeping the duty cycle fixed at 100%. All further experiments were acquired with a 100 ms ramp and 10 PASEF MS/MS scans per topN acquisition cycle, except for the Evosep One experiments, which were performed with four PASEF MS/MS scans per cycle. In TOF mass spectrometry, signal-to-noise ratios can conveniently be increased by summation of individual TOF scans. Here, low-abundance precursors with an intensity below a 'target value' were repeatedly scheduled for PASEF-MS/MS scans until the summed ion count reached the target value (e.g. four times for a precursor with the intensity 5000 arbitrary units (a.u.) and a target value of 20,000 a.u.). We set the target value to 20,000 a.u. for all methods, except for the Evosep One experiments where it was set to 24,000 a.u.

MS and MS/MS spectra were recorded from  $m/z$  100 to 1700. Suitable precursor ions for PASEF-MS/MS were selected in real time from TIMS-MS survey scans by a sophisticated PASEF scheduling algorithm (see also Results). A polygon filter was applied to the  $m/z$  and ion mobility plane to select features most likely representing peptide precursors rather than singly charged background ions. The

quadrupole isolation width was set to 2 Th for  $m/z < 700$  and 3 Th for  $m/z > 700$ , and the collision energy was ramped stepwise as a function of increasing ion mobility: 52 eV for 0–19% of the ramp time; 47 eV from 19–38%; 42 eV from 38–57%; 37 eV from 57–76%; and 32 eV for the remainder.

The TIMS elution voltage was calibrated linearly to obtain reduced ion mobility coefficients ( $1/K_0$ ) using three selected ions of the Agilent ESI-L Tuning Mix ( $m/z$  622, 922, 1222) (35).

Collisional cross sections were calculated from the Mason Schamp equation (36).

$$CCS = \frac{3ze}{16 K_0} \frac{1}{\sqrt{\frac{2\pi}{\mu k_b T}}}$$

where  $z$  is the charge of the ion,  $e$  is the elemental charge,  $k_b$  is Boltzman's constant,  $\mu$  is the reduced mass, and  $T$  the temperature (305 K). For all calculations, we assumed pure N<sub>2</sub> as the drift gas.

**Data Analysis**—Mass spectrometry raw files were processed with MaxQuant (37) version 1.6.1.13, which has been extended to incorporate the additional ion mobility dimension and adapted to handle the TIMS data format. This new version of MaxQuant is publicly available and will be described in detail separately (Cox and co-workers, *in preparation*). Briefly, it assembles four-dimensional isotope clusters - defined by  $m/z$ , retention time, ion mobility and intensity - from the TIMS-MS spectra and extracts ion mobility separated MS/MS spectra from the PASEF scans. Each MS/MS spectrum is assigned to its respective precursor ion by quadrupole isolation  $m/z$  and ion mobility values, and in case a precursor has been fragmented multiple times in one acquisition cycle, the respective spectra are collapsed to a single spectrum with increased signal-to-noise. For the four-dimensional feature detection in MaxQuant, only every third data point (TOF scan) in the TIMS dimension was considered ("TIMS step width" = 3), and the "TIMS half width" parameter was set to 4 TOF scans (equivalent to about 440  $\mu\text{s}$ ). The "TIMS mass resolution" parameter was set to 32,000 and MS/MS peaks with an intensity below 1.5 units were discarded.

The MS/MS spectra were matched to *in silico* derived fragment mass values of tryptic peptides from a reference proteome (Uniprot, 2016/05, HeLa: 91,618 entries including isoforms, *E. coli*: 4313 entries including isoforms) and 245 potential contaminants by the built-in Andromeda search engine (38). A maximum of two missing cleavages were allowed, the required minimum peptide sequence length was 7 amino acids, and the peptide mass was limited to a maximum of 4600 Da. Carbamidomethylation of cysteine residues was set as a fixed modification, and methionine oxidation and acetylation of protein N termini as variable modifications. The initial maximum mass tolerances were 70 ppm for precursor ions and 35 ppm for fragment ions. After re-calibration, precursor mass tolerances were individually adjusted by MaxQuant to less or equal 20 ppm for each isotope pattern based on the local precision of the mass measurement. We employed a reversed sequence library to control the false discovery rate (FDR) at less than 1% for peptide spectrum matches and protein group identifications.

Decoy database hits, proteins identified as potential contaminants, and proteins identified exclusively by one site modification were excluded from further analysis. Label-free protein quantification was performed with the MaxLFQ algorithm (39) requiring a minimum ratio count of 1. All other MaxQuant parameters were kept at their default values.

Mass spectrometric metadata, such as the information about PASEF-scheduled precursor ions, were directly accessed and extracted from the Bruker *.tbf* raw files with a SQLite database viewer (SQLite Manager, v0.8.3.1). Bioinformatic analysis and visualization was performed in either Python (Jupyter Notebook), Perseus (40) (v1.6.0.8) or the R statistical computing environment (41) (v3.2.1).

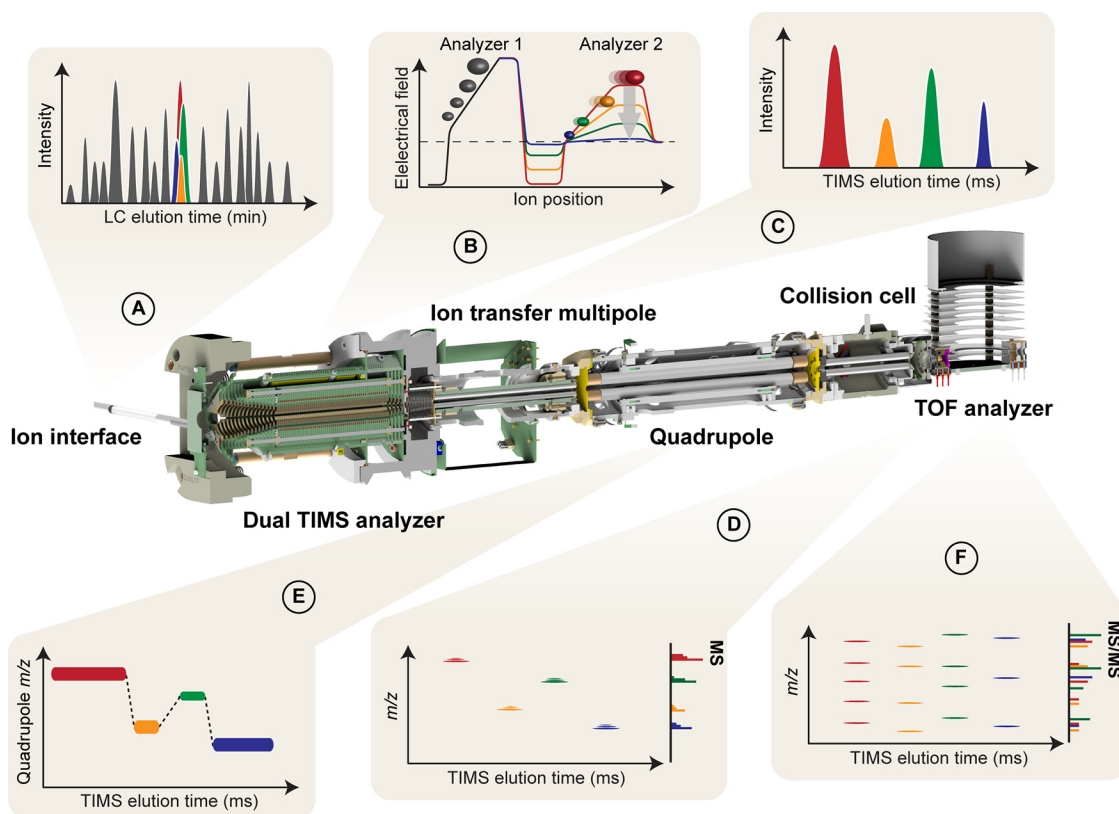


**FIG. 1. Online Parallel Accumulation - Serial Fragmentation (PASEF) with the timsTOF Pro.** *A*, Peptides eluting from the chromatographic column are ionized and enter the mass spectrometer through a glass capillary. *B*, In the dual Tims analyzer, the first Tims section traps and stores ion packets, and the second resolves them by mobility. *C*, *D*, Ion mobility separated ions are released sequentially from the second Tims analyzer as a function of decreasing electrical field strength and yield mobility-resolved mass spectra. *E*, In PASEF MS/MS scans, the Tims analyzer and the quadrupole are synchronized and the quadrupole isolation window switches within sub-milliseconds between mobility resolved precursor ions of different  $m/z$ . *F*, This yields multiple ion mobility resolved MS/MS spectra from a single Tims scan, and ensures that multiple trapped precursor ion species are used for fragmentation. Non mobility-resolved MS and MS/MS spectra are projected onto the right axes in (*E*) and (*F*) for comparison.

**Experimental Design and Statistical Rationale**—The complete data set reported in this study comprises 108 raw files. Samples were grouped by mass spectrometric acquisition methods or, in case of the data for Fig. 5, by pipetting ratios. Replicate injections were performed to assess the technical reproducibility of the respective methods and their quantitative accuracy. The exact  $N$  numbers are  $n = 4$  in Fig. 4;  $n = 4$  in Fig. 5A–5C;  $n = 5$  in Fig. 5D;  $n = 3$  in Fig. 6A–6B;  $n = 16$  in Fig. 6C;  $n = 4$  in Fig. 7A–7C and  $n = 1$  in Fig. 7D. To allow accurate external calibration of ion mobility values, we acquired experiments with different Tims ramp times in batches. Dilution series were measured from low to high concentrations starting with blank runs to avoid carry over. This study does not draw biological conclusions, which is why process and biological replicates or controls were not performed. In the description of Fig. 5D the data were filtered for at least two valid values in each group (1:1 and 1:5 mixing ratios, respectively) and a one-sided two-sample  $t$  test was performed. Multiple-hypothesis testing was corrected by truncating  $t$  test significant hits at a permutation-based FDR threshold of 0.05 (250 randomizations) in the Perseus software.

## RESULTS

**Construction of a Tims-QTOF Instrument with Online PASEF**—The timsTOF Pro is a quadrupole time-of-flight (QTOF) mass spectrometer equipped with a second generation

dual Tims analyzer in the first vacuum stage (Fig. 1). This set-up spatially separates ion accumulation and ion mobility analysis into two sequential sections of the Tims tunnel, so that these steps happen in parallel (28) (analyzer 1 and 2 in Fig. 1B). Within the limits of ion storage capacity, up to 100% of the ions that enter the mass spectrometer can therefore be utilized for mass analysis. Here, we typically accumulated ions for 25 to 200 ms, and transferred them into the second Tims region within 2 ms. From this Tims region they were released by decreasing the voltage gradient linearly within 25 to 200 ms (Tims ramp time). Simulations show that most of the ion mobility separation happens near the top plateau close to the exit of the device (42–44) and we observed that leaving peptide ion packets had narrow ion mobility peaks with median half widths of about 2 ms or less (Fig. 1C). In Tims, low mobility ions are released or ‘eluted’ first, followed by more mobile ions with smaller collisional cross sections relative to their charge. In addition to separating ions by shape and size, the time-focusing effect of Tims increases signal-to-noise ratios about 50-fold (depending on the relative accumulation and ramp times) compared with the standard

continuous acquisition mode because ion species are concentrated into narrow packets whereas the noise distributes across the ion mobility scan (28).

At the exit of the TIMS device, ions pass through the ion transfer multipole, the quadrupole mass filter and are then accelerated into the collision cell. From there, intact (MS scans) or fragment (MS/MS scans) ions are extracted into an orthogonal accelerator unit and pushed into the flight tube for mass analysis (Fig. 1D). The ions enter a V-shaped flight path through a two-stage reflectron and finally impinge on a multi-channel plate ion detector coupled to a 10-bit digitizer with a sampling rate of 5 Gigasamples/s, enabling high-resolution mass analysis ( $R > 35,000$ ). With time-of-flight mass analyzers, as opposed to Fourier-transform mass analyzers, this resolving power is nearly constant over the entire  $m/z$  range and independent of the scan time. Of note, we observed that the re-designed ion transfer path - presumably mainly the 90-degree bent at the entrance of the TIMS device and the new quadrupole with increased inner diameter - had a positive effect on the instrument's robustness. This was evidenced by continuous operation of the instrument during its development for more than 1.5 years, in which time we only cleaned the ion transfer capillary but not the internals of the instrument.

In PASEF mode, MS/MS precursor selection by the quadrupole mass filter is synchronized with the release of ions from the TIMS device, which requires very fast switching times of the quadrupole to keep pace with the fast ion mobility separation and to maximize the number of precursors per TIMS scan (Fig. 1E). The *timsTOF Pro* electronics have been designed to meet these requirements. RF and DC voltages for mass selection are now calculated and set by a real-time field-programmable array, as opposed to a conventional and slower serial interface. This allows fully synchronized operation of TIMS and quadrupole with switching times of 1 ms or less. By setting the quadrupole to  $N$  different isolation windows, PASEF yields  $N$  ion-mobility-resolved MS/MS spectra for a single TIMS scan (Fig. 1F). Because all precursor ions are stored in parallel, the absolute ion count per MS/MS spectrum is equal to a conventional TOF MS/MS spectrum summed up over the accumulation time, giving rise to an  $N$ -fold increase in sequencing speed without sacrificing sensitivity. The maximum number of precursors per TIMS scan is not limited by the instrument electronics, but rather by the separation of precursors in the ion mobility dimension and by the efficient design of "switching routes" for precursor selection, which will be described next.

**PASEF Precursor Selection in Real-time**—In complex proteomics samples, such as whole cell lysates, hundreds to thousands of peptides elute at any time, presenting a challenge for optimal precursor selection even with the 10-fold higher sequencing speed offered by PASEF. Fortunately, precursors are now distributed in a two-dimensional ( $m/z$  and ion mobility) space in which an optimal route can be selected, like the "traveling salesman problem" in computer science. Even

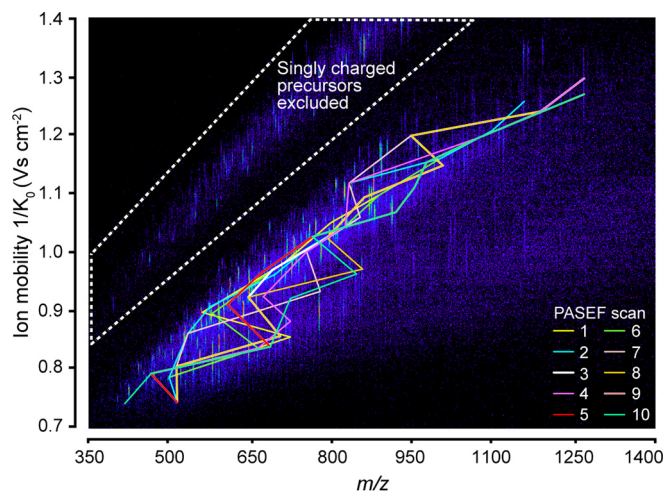
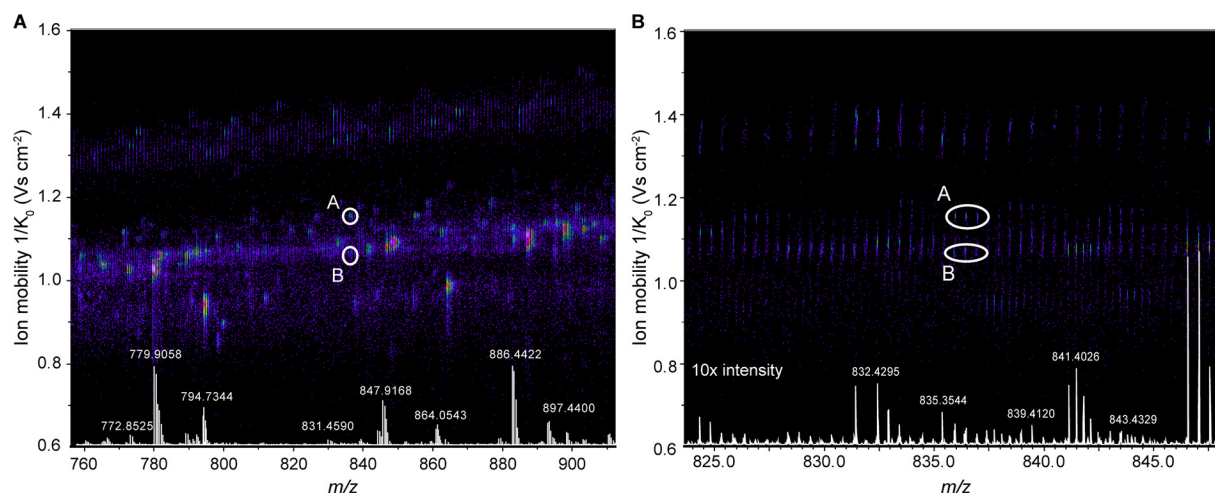


FIG. 2. **Real-time PASEF precursor selection in three dimensions.** Heat-map visualization of ion mobility resolved peptide ions at a single time point in an LC-TIMS-MS analysis of a HeLa digest. Connected lines indicate the  $m/z$  and mobility positions of all precursor ions selected for fragmentation in the following TIMS-PASEF scans (color-coded).

though exact solutions exist, for example by a brute-force method that simply iterates over all possible combinations, they cannot be computed on the LC time scale nor is it clear which peaks are most desirable to "visit". Instead, we here developed a heuristic algorithm that limits the computational time to about 100 ms in complex samples, and aims to maximize the number of precursors per acquisition cycle that can be successfully identified. This involves three dimensions: precursor  $m/z$ , signal intensity and ion mobility (Fig. 2). Our precursor search is offset by one acquisition cycle from ongoing data acquisition to avoid introducing any scan overhead time. In distributing precursors to PASEF scans, our algorithm accounts for the quadrupole switching time as well as the elution order of ion mobility peaks and prioritizes high-abundance precursors. In principle, the maximum coverage of eluting peptides should be achieved by using the PASEF speed advantage exclusively on unique precursor ions. However, this leads to many low abundant precursors being selected, and thus many low-quality MS/MS spectra. Common strategies to increase spectral quality are (1) increasing the ion accumulation time for selected, isolated ions (in trapping-based instruments) or (2) summing consecutive scans (in TOF-MS). In contrast, TIMS-PASEF accumulates all precursors upstream of selection whereas many precursors can be fragmented consecutively in each single PASEF scan. This enables deliberate and efficient re-scheduling of selected low-abundance precursor ions in subsequent PASEF scans. In post-processing, these individual spectra are summed to increase signal-to-noise. This "re-sequencing" is implemented in our precursor algorithm by a "target intensity" parameter, with which users can balance the desired spectral quality with the number of unique precursors. Other than that,



**FIG. 3. Trapped ion mobility separation of peptide precursor ions.** A, The two nearly isobaric peptide precursor ions A and B were distinguished by their ion mobility and selected separately for fragmentation by the PASEF scheduling algorithm in an LC-TIMS-MS experiment of a HeLa digest. B, Zoomed view into the precursor  $m/z$  range. Non mobility-resolved MS spectra are projected onto the lower axis for comparison. The corresponding MS/MS spectra are shown in [supplemental Fig. S1](#).

we excluded precursors dynamically after one sequencing event to not compromise proteomic depth. Singly charged species were readily excluded by their characteristic positions in the  $m/z$  versus ion mobility plane. The flow chart in [supplemental Fig. S1](#) depicts the precursor selection algorithm in detail.

We tested the performance of our precursor selection algorithm in 120 min LC-TIMS-MS runs of HeLa digests. Fig. 2 shows a representative TIMS-MS survey scan in the middle of the LC gradient. From this 100 ms TIMS scan, our algorithm selected 50 unique precursor ions for fragmentation in the subsequent PASEF scans (color-coded) out of which 32 low-abundance precursors were repeatedly sequenced. All precursor ions were widely distributed in  $m/z$  and ion mobility space, indicating an efficient coverage of the entire precursor space. In total, 118 MS/MS spectra were acquired in this cycle, which equals a sequencing rate of more than 100 Hz. Because all precursors were accumulated for 100 ms, the total number of ions for each precursor corresponds to that of a 10 Hz MS/MS selection if no PASEF had been employed.

With the selection algorithm in place, we inspected hundreds of precursor identifications in our data sets. Often, the separation of precursors along the additional ion mobility dimension was crucial as illustrated in Fig. 3. In a projection of the data onto the  $m/z$  axis, no obvious precursor signals were present, even when enlarging the signal 10-fold relatively to the more abundant peaks. However, the precursor selection algorithm had found and fragmented two distinct isotope clusters in the ion mobility -  $m/z$  space, which were separately fragmented by PASEF and clearly identified ([supplemental Fig. S2](#)).

**Single Run Proteomes**—Next, we investigated the effect of different TIMS ramp times on precursor selection. Given a minimum selection and transition time for the quadrupole adjustment of a few ms, the overall number of achievable fragmentation events should be roughly similar for different

TIMS ramp times as increasing ramp times allow fragmenting more precursors per PASEF scan - while acquiring less scans overall. To find a good balance for proteomics applications, we varied the TIMS ramp from 25 to 200 ms and kept the number of PASEF scans at 10 per acquisition cycle. We chose to operate the instrument at a near 100% duty cycle by setting the TIMS acquisition time equal to the ramp time.

With the slowest (and therefore highest mobility resolving) TIMS ramp, a median of 24 precursors were sequenced per scan (Fig. 4A). Faster ramp times resulted in nearly proportionately less precursors per PASEF scan, which was partially balanced by the overall higher number of scans per analysis. Interestingly, the 25 ms ramp was clearly inferior as it did not take full advantage of the PASEF principle, yielding only about 380,000 MS/MS spectra per run. With the 100 ms ramp over 600,000 MS/MS spectra were acquired in two hours (Fig. 4B). For comparison, acquiring the same number of MS/MS spectra without PASEF at the same sensitivity would have taken 11 times longer—almost 1 day. Remarkably, the instrument was sequencing at rates above 100 Hz during the entire time that peptides were eluting. As discussed above, we decided to use this extreme speed in part on resequencing low-abundance peptides to generate higher-quality summed spectra (Fig. 4C). On average, a given precursor ion was fragmented 2.2 times in 25 ms ramps and 1.9 times with 200 ms ramps. Overall, this resulted in up to 320,000 MS/MS spectra of unique precursor ions in a single run as detected by the real-time PASEF scheduling algorithm (Fig. 4D), although post-processing in MaxQuant combined many of these.

From 200 ng whole-cell HeLa digest per run, we identified on average 25,885 sequence-unique peptides in quadruplicate single runs with the 200 ms method, and about 32,000 with the faster 100 ms and 150 ms methods (Fig. 4E). The median peptide length was 14 amino acids. In all runs, the

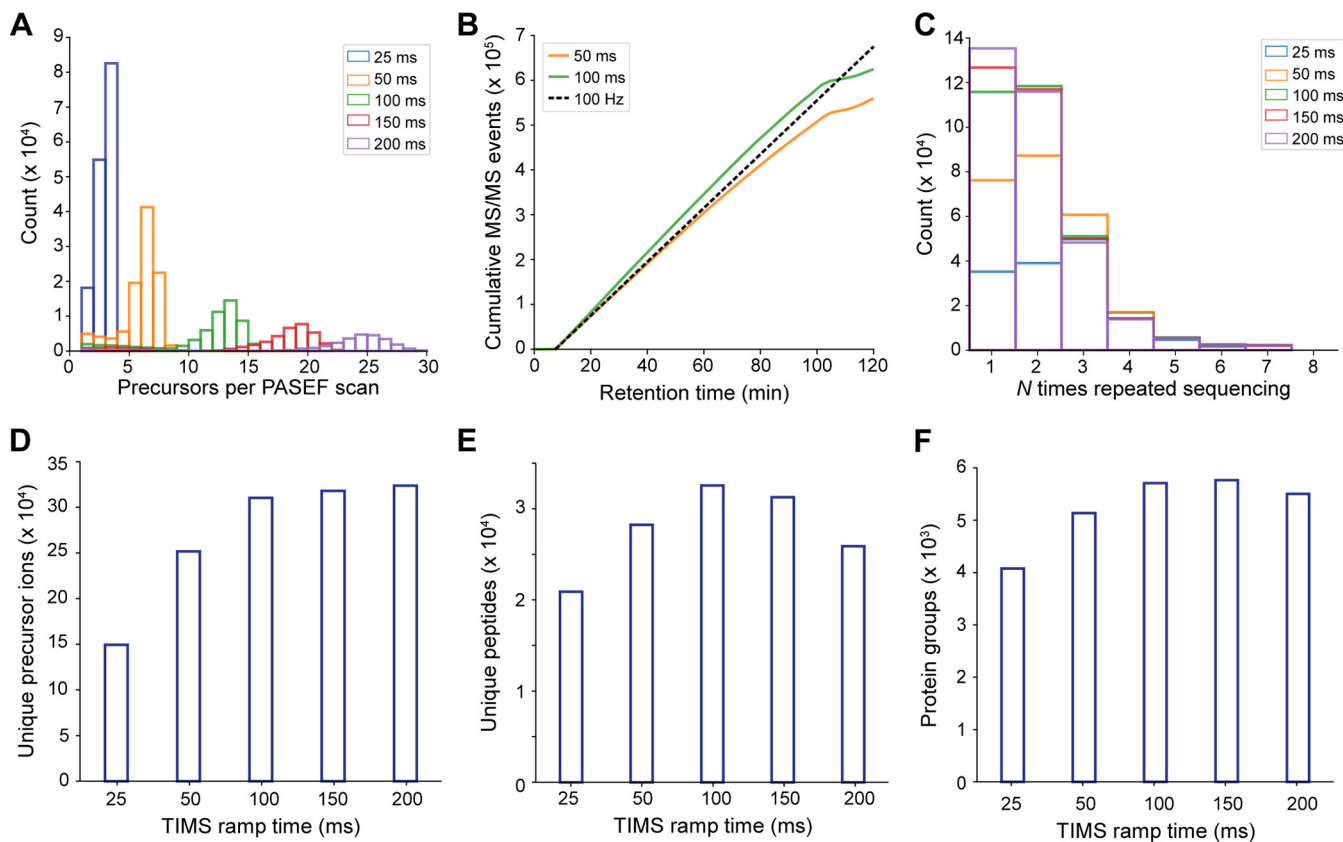


FIG. 4. **Single run analyses of a HeLa digest.** A, Number of selected precursor ions per PASEF scan with different TIMS ramp times in 120 min runs of 200 ng HeLa digests. B, Cumulative number of PASEF MS/MS spectra as a function of retention time for 50 ms and 100 ms TIMS ramps. The dashed line indicates the theoretical number of MS/MS spectra for a constant acquisition rate of 100 Hz starting at a retention time of 7.5 min. C, Number of repeated sequencing events for precursors with different ramp times. D, Number of unique precursor ions detected with different TIMS settings. E, Average number of sequence-unique peptides identified in single runs ( $n = 4$ ) with different TIMS settings. F, Average number of protein group identifications in single runs ( $n = 4$ ) with different TIMS settings.

median absolute peptide mass accuracy was below 1.5 ppm. The number of inferred protein groups at an FDR below 1% increased to an average of over 5700 protein groups per run at TIMS ramp times of 100 and 150 ms (Fig. 4F). With the 100 ms ramp, we identified in total 6090 protein groups (5230 with two or more peptides) with a median sequence coverage of 19.7%.

**Label-free Proteome Quantification**—A central task in proteomics is the accurate quantification of protein abundances across multiple biological samples. Label-free quantification (LFQ) is a popular method because of its simplicity and scalability to larger sample cohorts. Using the optimized 100 ms TIMS method we quantified on average 5575 protein groups in 2 h LC-MS time across quadruplicate injections. Run-to-run reproducibility was high with a median pairwise Pearson correlation coefficient of 0.979 between the four runs, with excellent linearity over four orders of magnitude in protein abundance (Fig. 5A). The median coefficients of variation (CVs) were 15.3% for the non-normalized peptide intensities and 7.2% at the protein level after MaxLFQ normalization (39) (Fig. 5B).

Quantitative accuracy in proteomics may be limited if proteins are inconsistently measured across the samples. In

data-dependent acquisition schemes, this is partially because of semi-stochastic precursor selection - a consequence of the large number of co-eluting precursor candidates and the finite sequencing speed. We asked if the severalfold faster PASEF method as compared with standard shotgun acquisition methods would improve this situation even without transferring identifications by precursor mass (“matching between runs”). Indeed, PASEF alleviated the “missing value” problem and provided quantification values for 4972 proteins in four out of four runs (Fig. 5C). Only 279 low-abundance proteins were exclusively quantified in a single replicate. This translated into a data completeness of 91.5%, which compares favorably to standard data-dependent acquisition and is similar to data-independent acquisition schemes. We expect that transferring identifications between runs, as with the MaxQuant matching between runs feature, will lead to even more consistent protein quantification across samples.

To further benchmark the quantitative accuracy of our setup, we mixed tryptic digests from HeLa and *Escherichia coli* in 1:1 and 1:5 ratios and measured each sample in quin-



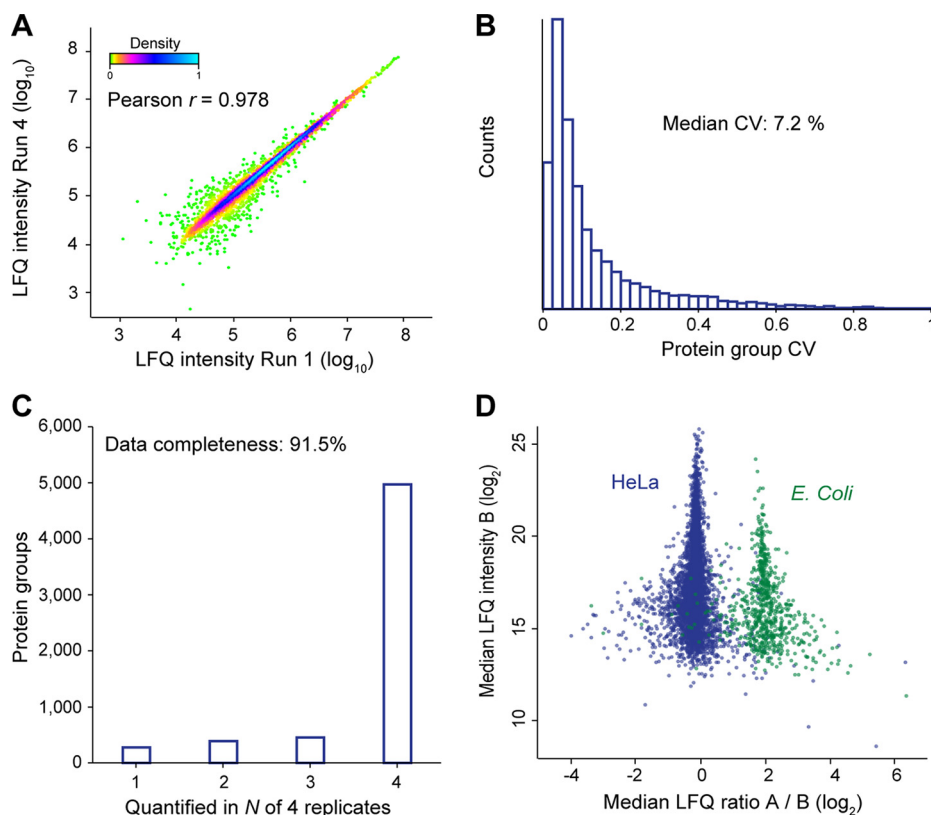


**FIG. 5. Label-free proteome quantification.** A, Pearson correlation of protein intensities in two replicate injections of a HeLa digest. B, Coefficients of variation (CVs) for protein quantities in four replicates ( $n = 5,811$ ). C, Number of proteins quantified in  $N$  out of four replicates. D, Label-free quantification benchmark with whole-cell HeLa and *E. coli* digests mixed in 1:1 and 1:5 ratios (wt:wt). The scatterplot shows the median fold-change of 5407 human and 728 *E. coli* proteins in quintuplicate single runs.

tuplicate 120 min single runs. Overall, we quantified 6135 protein groups (5407 HeLa; 728 *E. coli*) with at least one valid value for both mixing ratios. Plotting the median fold-changes yielded two distinct clouds for HeLa and *E. coli* proteins, which were 4.3-fold separated in abundance, slightly less than the intended 5-fold mixing ratio (Fig. 5D). Both populations were narrow ( $\sigma(\text{HeLa}) = 0.44$ ;  $\sigma(\text{E. coli}) = 0.77$ ) relative to the expected fold-change and they had minimal overlap. Considering only the 5686 proteins with at least two valid values for each mixing ratio (5052 HeLa, 634 *E. coli*), a one-sided Student's *t* test returned 602 significantly changing *E. coli* proteins at a permutation-based FDR below 0.05. This represents an excellent sensitivity of  $\sim 95\%$  and only 64 human proteins (1.3%) were falsely classified as changing. From these results, we conclude that the combination of TIMS and PASEF provides precise and accurate label-free protein quantification at a high level of data completeness.

**High Throughput and Limited Sample Amounts**—The performance characteristics discussed so far suggest that the instrument is particularly well suited for rapid and high sensitivity proteome analysis. To test this, we first reduced the peptide amount on column from 100 ng down to 10 ng HeLa digest per injection (Fig. 6A). With 100 ng on column and a 1 h gradient, we reproducibly identified 4513 protein groups, 79%

of the proteome coverage with 200 ng in half the measurement time. Out of these, 3294 protein groups were quantified with a CV below 20%. At 50 ng, we quantified 4215 protein groups with high quantitative accuracy (median CV 9.8%), motivating us to inject even lower sample amounts. Remarkably, from only 10 ng HeLa digest, we still identified 2723 protein groups on average and 3113 in total (2159 with two or more peptides in at least one replicate). Assuming 150 pg protein per cell (45), this corresponds to the total protein amount of only about 60 HeLa cells, suggesting that TIMS-PASEF is well suited to ultrasensitive applications in proteomics. Even at this miniscule sample amount, quantitative accuracy remained high with a median peptide intensity CV of 9.7% and 1841 proteins quantified at a CV < 20%.

To investigate achievable throughput, we repeated our sensitivity experiments with a 30 min gradient (Fig. 6B). This is an attractive strategy as steeper gradients compress the ion current in narrower LC elution peaks (about 7 s FWHM for the 120 min gradient *versus* 4 s FWHM for the 30 min gradient), thereby providing higher ion counts in individual MS/MS scans. This is also evident from the observation that the target value was reached within an average of 1.5 repeats as compared with 2.0 and 1.7 for the 120 and 60 min gradients. Because of the very high sequencing speed of PASEF, reducing the measurement

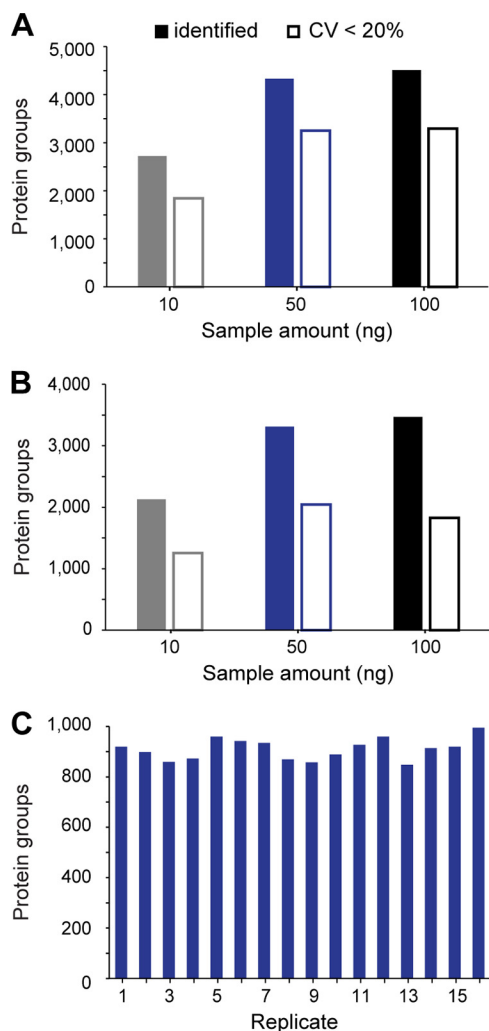


**FIG. 6. Rapid and sensitive HeLa proteome measurements.** A, Average number of protein groups identified and quantified with a CV < 20% in 60 min single runs ( $n = 3$ ). B, Average number of protein groups identified and quantified with a CV < 20% in 30 min single runs ( $n = 3$ ). C, Number of protein groups identified in sixteen replicate injections with the 5.6 min gradient.

time had only limited effect on proteome coverage. From 100 ng HeLa digest we identified on average 3470 protein groups in quadruplicate single runs, whereas 10 ng yielded 2128 protein groups, all with median CVs below 18%.

At the very short gradients made possible by the PASEF principle, throughput starts to be severely affected by the washing, loading and equilibration steps of the HPLC between injections. We therefore turned to the recently introduced Evosep One instrument, which features a preformed gradient, increasing robustness and largely eliminating idle time between injections (34). To explore the throughput limits of complex proteome analysis with PASEF, we made use of the “200 samples per day” method on the Evosep One, which consists of a 5.6 min gradient with 7.2 min total time between injections. Remarkably, in 16 replicates, 1231 proteins (910

with two or more peptides) were identified without any identification transfer from libraries and with only 50 ng of injected cell lysate (Fig. 6C). This combination of fast LC turnaround times with PASEF also holds great promise for rapid yet comprehensive analyses of less complex samples, for example protein interactomes, or the quantification of trace-level host cell proteins (HCPs) in recombinant biotherapeutics.

**Large-scale Measurement of Peptide Collisional Cross Sections**—In TIMS, the counteracting forces of a gas flow and an electrical field are used to separate the ions and to measure their mobility. Conceptually, this closely resembles the (inverted) situation in drift tube ion mobility, where ions are dragged by an electrical field through resting gas molecules. Because the underlying physics is identical, TIMS measurements are expected to correlate directly with classical drift tube ion mobility measurements and this has been established experimentally by Park and colleagues (42). Therefore, in contrast to other ion mobility setups (24), such as traveling-wave ion mobility (46) and differential ion mobility (47), TIMS can directly determine collisional cross sections by internal or external calibration.

We reasoned that the rapid measurement of tens of thousands of peptides demonstrated above, in combination with accurate CCS measurements, should allow generating a large-scale overview of the CCS dimension of peptides. We first explored the reproducibility with repeated injections of HeLa digest. Before the first injection, we calibrated the ion mobility dimension using reduced ion mobility values ( $1/K_0$ ;  $V \cdot s \cdot cm^{-2}$ ) of phosphazine derivatives from the literature (35), which can be converted to  $TIMS$  CCS values using the Mason-Schamp equation (Experimental Procedures). Peptide ions can occur in multiple conformations (e.g. proline-containing peptides (48)), which results in multiple ion mobility peaks and complicates the analysis. For simplicity, we here only considered the most abundant feature reported by MaxQuant.

In four replicates, we generated 23,738  $1/K_0$  values of commonly identified peptide ions in all runs with a median CV of 0.1% and a median pairwise correlation coefficient > 0.99 (Fig. 7A). The average absolute deviation of  $TIMS$  CCS values across all four replicates was 0.2% (Fig. 7B). In our hands, this is at least 10-fold more reproducible than LC retention time, even on the same column and with the same gradient. Interestingly, the  $TIMS$  CCS measurements were also highly transferable across different TIMS ramp times (100 and 200 ms) as evident from a Pearson correlation coefficient of > 0.99 between them (Fig. 7C).

Having established precise  $TIMS$  CCS measurements in single runs, we next used loss-less high pH fractionation (33) to extend the scale of our data set. Measuring 48 fractions with 2 h gradients each resulted in 129,110  $TIMS$  CCS values (filtered for  $z > 1$ ) from 101,420 unique peptide sequences and about 9400 protein groups. In the  $m/z$  versus  $TIMS$  CCS plot, doubly, triply and higher-charged populations are clearly separated (Fig. 7D, Supplemental Table S1). Within each charge

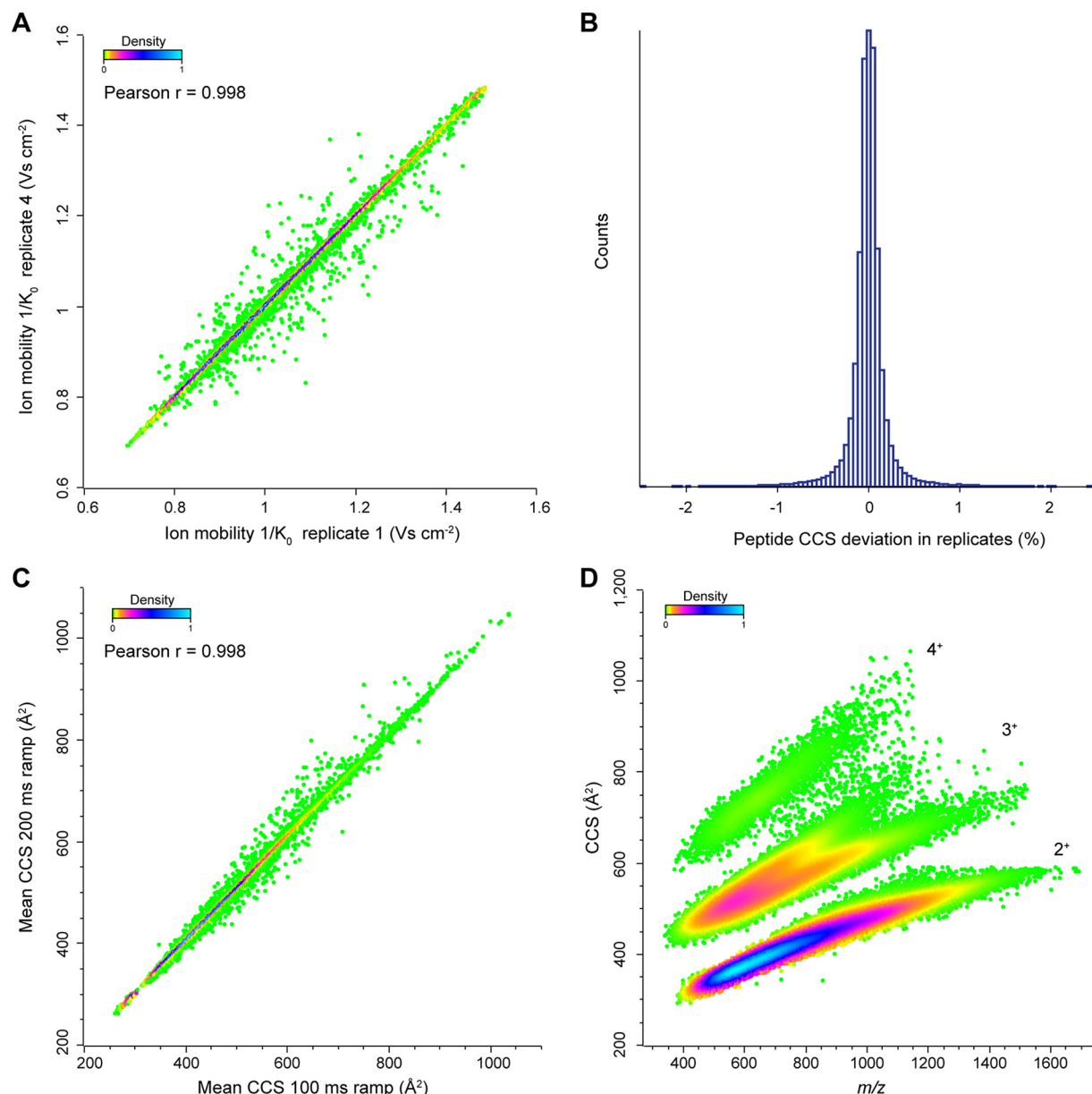


FIG. 7. **Large-scale and high-precision CCS measurements.** A, Pearson correlation of peptide ion mobilities in two replicate injections of a HeLa digest (100 ms TIMS ramps). B, Relative deviations of  $^{TIMS}CCS$  values of all individual peptides from their mean of quadruplicate LC-MS runs ( $n = 144,363$ ; 1,186 out of range). C, Pearson correlation of measured  $^{TIMS}CCS$  values in two injections of a HeLa digest with different TIMS ramp times (100 and 200 ms TIMS ramps). D, Density distribution of 129,110  $^{TIMS}CCS$  values from human tryptic peptide ions as a function of  $m/z$ . The main populations are annotated with their respective charge states.

state, there is clear correlation between  $m/z$  and cross section and triply charged species split into two prominent subpopulations, as expected from the literature (49–51). However, the precision of the  $^{TIMS}CCS$  determination is still more than 10-fold higher than the width of the ion mobility distribution for a given  $m/z$ . This results in additional peptide information that can be used for matching and identification.

#### DISCUSSION

Here, we have described the construction and evaluated the performance of a state-of-the-art quadrupole time-of-

flight instrument with a trapped ion mobility device and deep integration of the PASEF principle. The novel Bruker *timstOF Pro* successfully incorporates these building blocks in a robust and flexible manner, not only enabling shotgun-based PASEF operation but many other operation modes, which are still left to be explored.

The full implementation of PASEF in the hard- and firmware in an online format achieved results almost completely in line with those modeled and extrapolated from a laboratory prototype in our 2015 paper (31). This suggests that the physical

operating principles are indeed directly translatable to proteomics workflows. In particular, the instrument routinely delivers sequencing rates above 100 Hz in complex proteome samples. In standard MS/MS acquisition schemes, such high fragmentation rates inevitably imply very short ion collection times and consequently poor spectrum quality. In contrast, PASEF leverages the full scan speed of TOF instruments with undiminished sensitivity as precursor ions are trapped and released as condensed ion packages by the time they are selected for fragmentation. This enabled the identification of about 6000 protein groups in single runs from a human cancer cell line with minimal input material, and with high quantitative accuracy.

Although we focused on label-free quantification in the current study, we expect that the high number of spectra per run will particularly benefit MS/MS-based quantification methods, for example isobaric labeling with TMT (52), iTRAQ (53) or EASI-tag (54). These approaches should additionally benefit from the ion mobility separation itself as it increases the purity of the isolation window and thereby reduces potential artifacts from co-eluting and co-isolated precursor ions.

The high speed and sensitivity of the *timsTOF Pro* allowed us to drastically decrease both measurement time and sample amount, which culminated in the identification of about 2100 proteins from only 10 ng HeLa digest in 30 min. This makes the instrument very attractive for proteomics studies with extremely low starting amounts, for example micro-dissected tumor biopsies, and for high throughput clinical applications of proteomics, in combination with robust and fast LC systems.

Finally, we demonstrated that TIMS-PASEF provides an efficient way to generate comprehensive libraries of peptide collisional cross sections, much beyond past reports (51). Such large-scale measurements could contribute to elucidating fundamental properties of modified and unmodified peptide ions in the gas phase and may eventually enable the *in silico* prediction of CCS values by deep learning algorithms. Furthermore, the very high precision of the CCS measurements with TIMS demonstrated here opens new avenues for spectral library-based identifications, in which the CCS parameter adds important evidence either on the MS level or, in data-independent acquisition strategies, also on the MS/MS level.

We conclude that the *timsTOF Pro* is a high-performance addition to the technology toolbox in proteomics, with many added opportunities enabled by TIMS-PASEF.

**Acknowledgments**—We thank our colleagues in the department of Proteomics and Signal Transduction and at Bruker Bremen and Bruker Billerica for discussion and help, in particular Drs. P. Geyer and I. Paron.

#### DATA AVAILABILITY

The raw datasets and the MaxQuant output files generated and analyzed throughout this study have been deposited at the ProteomeXchange Consortium via the PRIDE partner repository (55) with the dataset identifier PXD010012 (<https://www.ebi.ac.uk/pride/archive/>). MaxQuant *msms.txt* and *.apl*

files are provided for viewing of annotated spectra, including spectra of single peptide protein identifications.

\* This work was partially supported by the German Research Foundation (DFG-Gottfried Wilhelm Leibniz Prize) granted to Matthias Mann and by the Max-Planck Society for the Advancement of Science.

§ This article contains [supplemental Figures and Table](#). The authors state that they have potential conflicts of interest regarding this work: S.K., H.K., M.L., M.K., N.G., J.D. M.P. and O. R. are employees of Bruker, the manufacturer of the *timsTOF Pro*. O.H. and N.B. are employees of Evosep. M.M. is an indirect investor in Evosep.

§§ To whom correspondence should be addressed: Proteomics and Signal Transduction, Max Planck Institute of Biochemistry, Am Klopferspitz 18, 82152 Martinsried, Germany. Tel.: +49 89 8578-2557; Fax: +49 89 8578-2412; E-mail: [mmann@biochem.mpg.de](mailto:mmann@biochem.mpg.de).

Author contributions: F.M., M.A.P., J.C., O.R., and M.M. designed research; F.M., A.-D.B., S.K., H.K., M.L., M.K., N.G., J.D., T.K., N.B., O.H., J.C., and O.R. performed research; F.M., A.-D.B., S.K., H.K., M.L., O.R., and M.M. analyzed data; F.M. and M.M. wrote the paper; N.B., O.H., and J.C. contributed new reagents/analytic tools.

#### REFERENCES

- Altelaar, A. F. M., Munoz, J., and Heck, A. J. R. (2012) Next-generation proteomics: towards an integrative view of proteome dynamics. *Nat. Rev. Genet.* **14**, 35–48
- Larance, M., and Lamond, A. I. (2015) Multidimensional proteomics for cell biology. *Nat. Rev. Mol. Cell Biol.* **16**, 269–280
- Aebersold, R., and Mann, M. (2016) Mass-spectrometric exploration of proteome structure and function. *Nature* **537**, 347–355
- Bekker-Jensen, D. B., Kelstrup, C. D., Batth, T. S., Larsen, S. C., Haldrup, C., Bramsen, J. B., Sørensen, K. D., Høyer, S., Ørntoft, T. F., Andersen, C. L., Nielsen, M. L., and Olsen, J. V. (2017) An Optimized Shotgun Strategy for the Rapid Generation of Comprehensive Human Proteomes. *Cell Syst.* **4**, 587–599.e4
- Michalski, A., Cox, J., and Mann, M. (2011) More than 100,000 detectable peptide species elute in single shotgun proteomics runs but the majority is inaccessible to data-dependent LC-MS/MS. *J. Proteome Res.* **10**, 1785–1793
- Aebersold, R., and Mann, M. (2003) Mass spectrometry-based proteomics. *Nature* **422**, 198–207
- Eliuk, S., and Makarov, A. (2015) Evolution of Orbitrap Mass Spectrometry Instrumentation. *Annu. Rev. Anal. Chem.* **8**, 61–80
- Domon, B., and Aebersold, R. (2006) Mass spectrometry and protein analysis. *Science* **312**, 212–217
- Han, X., Aslanian, A., and Yates, J. R. (2008) Mass spectrometry for proteomics. *Curr. Opin. Chem. Biol.* **12**, 483–490
- Beck, S., Michalski, A., Raether, O., Lubeck, M., Kaspar, S., Goedecke, N., Baessmann, C., Hornburg, D., Meier, F., Paron, I., Kulak, N. A., Cox, J., and Mann, M. (2015) The Impact II, a very high-resolution quadrupole time-of-flight instrument (QTOF) for deep shotgun proteomics. *Mol. Cell. Proteomics* **14**, 2014–2029
- Kanu, A. B., Dwivedi, P., Tam, M., Matz, L., and Hill, H. H. (2008) Ion mobility-mass spectrometry. *J. Mass Spectrom.* **43**, 1–22
- Cumeras, R., Figueras, E., Davis, C. E., Baumbach, J. I., and Gràcia, I. (2015) Review on Ion Mobility Spectrometry. Part 2: hyphenated methods and effects of experimental parameters. *Analyst* **140**, 1391–1410
- May, J. C., and McLean, J. A. (2015) Ion mobility-mass spectrometry: time-dispersive instrumentation. *Anal. Chem.* **87**, 1422–1436
- Eiceman, G. A., Karpas, Z., and Hill, H. H. J. (2013) *Ion Mobility Spectrometry* (CRC Press). 3rd Ed.
- Valentine, S. J., Counterman, A. E., Hoaglund, C. S., Reilly, J. P., and Clemmer, D. E. (1998) Gas-phase separations of protease digests. *J. Am. Soc. Mass Spectrom.* **9**, 1213–1216
- Srebalus Barnes, C. A., Hilderbrand, A. E., Valentine, S. J., and Clemmer, D. E. (2002) Resolving isomeric peptide mixtures: A combined HPLC/ion mobility-TOFMS analysis of a 4000-component combinatorial library. *Anal. Chem.* **74**, 26–36
- Ewing, M. A., Glover, M. S., and Clemmer, D. E. (2015) Hybrid ion mobility and mass spectrometry as a separation tool. *J. Chromatogr. A*, 27–29

18. Lanucara, F., Holman, S. W., Gray, C. J., and Eyers, C. E. (2014) The power of ion mobility-mass spectrometry for structural characterization and the study of conformational dynamics. *Nat. Chem.* **6**, 281–294
19. Valentine, S. J., Plasencia, M. D., Liu, X., Krishnan, M., Naylor, S., Udseth, H. R., Smith, R. D., and Clemmer, D. E. (2006) Toward plasma proteome profiling with ion mobility-mass spectrometry. *J. Proteome Res.* **5**, 2977–2984
20. Baker, E. S., Livesay, E. A., Orton, D. J., Moore, R. J., Danielson, W. F., Prior, D. C., Ibrahim, Y. M., LaMarche, B. L., Mayampurath, A. M., Schepmoes, A. A., Hopkins, D. F., Tang, K., Smith, R. D., and Belov, M. E. (2010) An LC-IMS-MS platform providing increased dynamic range for high-throughput proteomic studies. *J. Proteome Res.* **9**, 997–1006
21. Geromanos, S. J., Hughes, C., Ciavardini, S., Vissers, J. P. C., and Langridge, J. I. (2012) Using ion purity scores for enhancing quantitative accuracy and precision in complex proteomics samples. *Anal. Bioanal. Chem.* **404**, 1127–1139
22. Helm, D., Vissers, J. P. C., Hughes, C. J., Hahne, H., Ruprecht, B., Pachi, F., Grzyb, A., Richardson, K., Wildgoose, J., Maier, S. K., Marx, H., Wilhelm, M. E., Becher, I., Lemeer, S., Bantscheff, M., Langridge, J. I., and Kuster, B. (2014) Ion mobility tandem mass spectrometry enhances performance of bottom-up proteomics. *Mol. Cell. Proteomics* **13**, 3709–3715
23. Distler, U., Kuharev, J., Navarro, P., Levin, Y., Schild, H., and Tenzer, S. (2014) Drift time-specific collision energies enable deep-coverage data-independent acquisition proteomics. *Nat. Methods* **11**, 167–170
24. Cumeras, R., Figueras, E., Davis, C. E., Baumbach, J. I., and Gràcia, I. (2015) Review on Ion Mobility Spectrometry. Part 1: current instrumentation. *Analyst* **140**, 1376–1390
25. Fernandez-Lima, F. A., Kaplan, D. A., and Park, M. A. (2011) Note: Integration of trapped ion mobility spectrometry with mass spectrometry. *Rev. Sci. Instrum.* **82**, 126106
26. Fernandez-Lima, F., Kaplan, D. A., Suetering, J., and Park, M. A. (2011) Gas-phase separation using a trapped ion mobility spectrometer. *Int. J. Ion Mobil. Spectrom.* **14**, 93–98
27. Ridgeway, M. E., Lubeck, M., Jordens, J., Mann, M., and Park, M. A. (2018) Trapped ion mobility spectrometry: A short review. *Int. J. Mass Spectrom.* **425**, 22–35
28. Silveira, J. A., Ridgeway, M. E., Laukien, F. H., Mann, M., and Park, M. A. (2017) Parallel accumulation for 100% duty cycle trapped ion mobility-mass spectrometry. *Int. J. Mass Spectrom.* **413**, 168–175
29. Silveira, J. A., Ridgeway, M. E., and Park, M. A. (2014) High resolution trapped ion mobility spectrometry of peptides. *Anal. Chem.* **86**, 5624–5627
30. Ridgeway, M. E., Silveira, J. A., Meier, J. E., and Park, M. A. (2015) Micro-heterogeneity within conformational states of ubiquitin revealed by high resolution trapped ion mobility spectrometry. *Analyst* **140**, 6964–6972
31. Meier, F., Beck, S., Grassl, N., Lubeck, M., Park, M. A., Raether, O., and Mann, M. (2015) Parallel accumulation–serial fragmentation (PASEF): multiplying sequencing speed and sensitivity by synchronized scans in a trapped ion mobility device. *J. Proteome Res.* **14**, 5378–5387
32. Kulak, N. A., Pichler, G., Paron, I., Nagaraj, N., and Mann, M. (2014) Minimal, encapsulated proteomic-sample processing applied to copy-number estimation in eukaryotic cells. *Nat. Methods* **11**, 319–324
33. Kulak, N. A., Geyer, P. E., and Mann, M. (2017) Loss-less nano-fractionator for high sensitivity, high coverage proteomics. *Mol. Cell. Proteomics*, mcp.O116.065136
34. Bache, N., Geyer, P. E., Bekker-Jensen, D. B., Hoerning, O., Falkenby, L., Treit, P. V., Doll, S., Paron, I., Müller, J. B., Meier, F., Olsen, J. V., Vorm, O., and Mann, M. (2018) A novel LC system embeds analytes in pre-formed gradients for rapid, ultra-robust proteomics. *Mol. Cell. Proteomics*, mcp.TIR118.000853
35. Stow, S. M., Causon, T. J., Zheng, X., Kurulugama, R. T., Mairinger, T., May, J. C., Rennie, E. E., Baker, E. S., Smith, R. D., McLean, J. A., Hann, S., and Fjeldsted, J. C. (2017) An interlaboratory evaluation of drift tube ion mobility-mass spectrometry collision cross section measurements. *Anal. Chem.* **89**, 9048–9055
36. Mason, E. A., and McDaniel, E. W. (1988) *Transport Properties of Ions in Gases* (John Wiley & Sons, Inc., New York, NY)
37. Cox, J., and Mann, M. (2008) MaxQuant enables high peptide identification rates, individualized p.p.b.-range mass accuracies and proteome-wide protein quantification. *Nat. Biotechnol.* **26**, 1367–1372
38. Cox, J., Neuhauser, N., Michalski, A., Scheltema, R. A., Olsen, J. V., and Mann, M. (2011) Andromeda: A peptide search engine integrated into the MaxQuant environment. *J. Proteome Res.* **10**, 1794–1805
39. Cox, J., Hein, M. Y., Luber, C. A., Paron, I., Nagaraj, N., and Mann, M. (2014) MaxLFQ allows accurate proteome-wide label-free quantification by delayed normalization and maximal peptide ratio extraction. *Mol. Cell. Proteomics*, M113.031591
40. Tyanova, S., Temu, T., Sinitcyn, P., Carlson, A., Hein, M. Y., Geiger, T., Mann, M., and Cox, J. (2016) The Perseus computational platform for comprehensive analysis of (prote)omics data. *Nat. Methods* **13**, 731–740
41. R Development Core Team. (2008) *R: A Language and Environment for Statistical Computing* (R Foundation for Statistical Computing, Vienna, Austria)
42. Michelmann, K., Silveira, J. A., Ridgeway, M. E., and Park, M. A. (2014) Fundamentals of trapped ion mobility spectrometry. *J. Am. Soc. Mass Spectrom.* **26**, 14–24
43. Silveira, J. A., Michelmann, K., Ridgeway, M. E., and Park, M. A. (2016) Fundamentals of trapped ion mobility spectrometry Part II: fluid dynamics. *J. Am. Soc. Mass Spectrom.* **27**, 585–595
44. Hernandez, D. R., Debord, J. D., Ridgeway, M. E., Kaplan, D. A., Park, M. A., and Fernandez-Lima, F. (2014) Ion dynamics in a trapped ion mobility spectrometer. *Analyst* **139**, 1913–1921
45. Volpe, P., and Eremenko-Volpe, T. (1970) Quantitative studies on cell proteins in suspension cultures. *Eur J Biochem* **12**, 195–200
46. Shvartsburg, A. A., and Smith, R. D. (2008) Fundamentals of traveling wave ion mobility spectrometry. *Anal. Chem.* **80**, 9689–9699
47. Buryakov, I. A., Krylov, E. V., Nazarov, E. G., and Rasulev, U. K. (1993) A new method of separation of multi-atomic ions by mobility at atmospheric pressure using a high-frequency amplitude-asymmetric strong electric field. *Int. J. Mass Spectrom. Ion Process.* **128**, 143–148
48. Counterman, A. E., and Clemmer, D. E. (2002) Cis-Trans Signatures of Proline-Containing Tryptic Peptides in the Gas Phase. *Anal. Chem.* **74**, 1946–1951
49. Valentine, S. J., Counterman, A. E., and Clemmer, D. E. (1999) A database of 660 peptide ion cross sections: use of intrinsic size parameters for bona fide predictions of cross sections. *J. Am. Soc. Mass Spectrom.* **10**, 1188–1211
50. Lietz, C. B., Yu, Q., and Li, L. (2014) Large-scale collision cross-section profiling on a traveling wave ion mobility mass spectrometer. *J. Am. Soc. Mass Spectrom.* **25**, 2009–2019
51. May, J. C., Morris, C. B., and McLean, J. A. (2017) Ion mobility collision cross section compendium. *Anal. Chem.* **89**, 1032–1044
52. Thompson, A., Schäfer, J., Kuhn, K., Kienle, S., Schwarz, J., Schmidt, G., Neumann, T., and Hamon, C. (2003) Tandem mass tags: A novel quantification strategy for comparative analysis of complex protein mixtures by MS/MS. *Anal. Chem.* **75**, 1895–1904
53. Ross, P. L., Huang, Y. N., Marchese, J. N., Williamson, B., Parker, K., Hattari, S., Khainovski, N., Pillai, S., Dey, S., Daniels, S., Purkayastha, S., Juhasz, P., Martin, S., Bartlett-Jones, M., He, F., Jacobson, A., and Pappin, D. J. (2004) Multiplexed protein quantitation in *Saccharomyces cerevisiae* using amine-reactive isobaric tagging reagents. *Mol. Cell. Proteomics* **3**, 1154–1169
54. Virreira Winter, S., Meier, F., Wichmann, C., Cox, J., Mann, M., and Meissner, F. (2018) EASI-tag enables accurate multiplexed and interference-free MS2-based proteome quantification. *Nat. Methods* **15**, 527–530
55. Vizcaino, J. A., Csordas, A., Del-Toro, N., Dianes, J. A., Griss, J., Lavidas, I., Mayer, G., Perez-Riverol, Y., Reisinger, F., Tertent, T., Xu, Q.-W., Wang, R., and Hermjakob, H. (2016) 2016 update of the PRIDE database and its related tools. *Nucleic Acids Res.* **44**, D447–D56